Journal of Chromatography, 282 (1983) 41–58
Elsevier Science Publishers B.V., Amsterdam — Printed in The Netherlands

CHROMSYMP. 152

HEAT-INDUCED STRUCTURAL CHANGES IN THE LICHROSORB RP-18–WATER HIGH-PERFORMANCE LIQUID CHROMATOGRAPHIC SYSTEM AND THEIR IMPACT ON THE THERMODYNAMIC ADSORPTION DATA OF BENZENE, NITROBENZENE AND PHENOL

W. E. HAMMERS* and P. B. A. VERSCHOOR
Laboratory for Analytical Chemistry, State University, Croesestraat 77A, 3522 AD Utrecht (The Netherlands)

SUMMARY

Capacity ratio (k) data of benzene, nitrobenzene and phenol have been measured on LiChrosorb RP-18 with water as the eluent at temperatures between 5 and 85°C. The influence of temperature on the structure of the RP-18 layer is discussed. Partial molar free energies, entropies, enthalpies and heat capacities of adsorption have been computed as a function of temperature by fitting Taylor's series expansions to the ln k data. These thermodynamic data appear to depend on (alterations of) the structure of the RP-18 layer. The effects of cavity formation and of hydrophobic hydration of benzene in water, and of the solute polarity on the strength of the adsorption, are discussed. It is shown that enthalpy/entropy compensation effects play an important, although not readily predictable, rôle in solute adsorption.

INTRODUCTION

The influence of temperature on solute retention in reversed-phase high-performance liquid chromatographic (RP-HPLC) systems has received relatively little attention. This may be due to the fact that a change of the column temperature generally has only a small effect on the selectivity. Therefore, separations are usually improved by optimizing the eluent composition. Moreover, the logarithm of the capacity ratio, k, in aqueous binary eluents is approximately linearly dependent on the reciprocal of the absolute temperature[1–5]. Therefore, from a practical point of view, research on temperature effects in RP-HPLC is not an urgent task.

On the other hand, the retention mechanism in RP-HPLC is still a controversial topic, and progress in this field may be achieved by more detailed investigations on temperature effects. This has been attempted by studying enthalpy–entropy (or enthalpy–reduced free energy) correlations[5–9]. Such studies require precise retention data and a suitable computer program to evaluate adsorption enthalpies and their errors as a function of temperature. A disadvantage of this approach is that contributions to the enthalpy will affect the entropy as well. As a result, they will be masked to some extent in such correlations. For that reason, a straightforward interpretation

0021-9673/83/$03.00

of enthalpy (and entropy) data seems preferable. Unfortunately, current adsorption models appear to be either inaccurate, or they are not readily applicable[10]. A possible alternative might be to account explicitly for the excess data of the solute in the eluent bulk. Along these lines, further insight into the interactions of the solute at the interface between the bonded phase and the eluent can be expected, as illustrated previously[10] on the basis of (reduced) free energies of adsorption. This approach is now extended to the adsorption enthalpies and heat capacities of benzene.

As this paper deals with the adsorption of only three solutes, *viz.*, benzene, nitrobenzene and phenol, in only one, rather outstanding system (LiChrosorb RP-18–water), its scope is limited. The choice of this particular system is based on the following considerations. First, it is probably one of the simplest systems. When aqueous binary eluents are used, a rigorous interpretation of the thermodynamic sorption data should account for the variation of the excess amount of (ad)sorbed eluent[11] with temperature, which will be rather laborious. Secondly, it may be a useful system for the examination of hydrophobic interactions in water or aqueous electrolyte solutions. In that case, the k values should not be affected by alterations in the structure of the bonded phase. Gilpin and Squires[12] suggested that such phase changes or transitions do not occur after a heat treatment of laboratory-prepared octyl, nonyl and decyl silicas in water and are absent altogether from octadecyl silica[13]. This conclusion seems to be based on the linear ln k *versus* $1/T$ plots obtained. In our opinion, this argument is not self-evident. In general, it is not expected that partial molar heat capacities of adsorption are equal to zero in such systems. For that reason, it seems worthwhile to examine the effects on k values of structural changes in non-polar bonded phases in more detail. Thirdly, LiChrosorb RP-18 was chosen as adsorbent because of its large surface concentration of bound octadecyl groups, effectively preventing adsorption to residual silanol groups on the silica surface underneath[10,14]. This will facilitate the description of the retention behaviour of solutes of various polarities.

THEORETICAL

If water is used as eluent and we assume that adsorption to residual silanol groups can be ignored, the retention volume of ^2H_2O (corrected for hold-up outside the column) is given by

$$V_{R,^2H_2O} = V_w \tag{1}$$

where V_w is the total volume of water in the column. When we are dealing with solute partitioning between the RP-18 phase and the eluent, a capacity ratio, k_i^*, can be defined by

$$k_i^* \equiv (V_{R,i} - V_{R,^2H_2O})/V_{R,^2H_2O} \tag{2}$$

wherein $V_{R,i}$ is the corrected retention volume of solute i. However, it will be argued below that solute molecules are essentially retained by adsorption in the interfacial layer between RP-18 and water. Therefore, we adopted a monolayer displacement adsorption model which implies that one monolayer of stagnant water, volume V_w,

covers the adsorbent phase. Consequently, the volume of the mobile phase in the column is $V_m = V_w - \bar{V}_w$. According to this model[10]:

$$k_i \equiv (V_{R,i} - V_m)/V_m = \bar{n}_i/n_i = (\bar{x}_i/x_i)\,(\bar{V}_w/V_m)$$
$$= (\gamma_i^{\infty}/\gamma_{i,\text{interf.}}^{\infty})\,(\bar{V}_w/V_m) \tag{3}$$

In this equation, $\bar{n}_i$ and n_i are the numbers of moles of i in the stagnant interfacial water layer and in the mobile eluent, respectively. The corresponding mole fractions are denoted by $\bar{x}_i$ and x_i, and the activity coefficients by $\gamma_{i,\text{interf.}}^{\infty}$ and γ_i^{∞}, respectively. Unfortunately, V_m cannot be experimentally determined, because inert solutes, *i.e.*, with $k = 0$ in eqn. 3, do not exist. Moreover, V_m cannot be accurately estimated, because $\bar{V}_w$ is not precisely known for bonded phases. It is doubtful whether their BET surface areas at 78°K are applicable at ambient temperature. Therefore, k_i has to be replaced by k_i^*. As $\bar{V}_w/V_w \ll 1$, combination of eqns. 1–3 gives:

$$\ln (\bar{x}_i/x_i) = \ln k_i^* + \bar{V}_w/k_i^* V_w - \ln (\bar{V}_w/V_w) \tag{4}$$

Because the RP-18 layer is not completely wetted by water, it can be estimated from the data given in the next section that $\bar{V}_w/V_w \lesssim 0.04$ in our column. This implies that the second term of the right-hand side of eqn. 4 can be omitted, provided that $k^* \gtrsim 4$. This condition is amply met in this work. Therefore, according to the monolayer adsorption model, the partial molar free energy, entropy and enthalpy of adsorption are evaluated from:

$$\Delta\bar{G}_a \equiv -RT \ln (\bar{x}_i/x_i) = -RT \ln k_i^* + RT\,\beta \tag{5}$$

$$\Delta\bar{S}_a = R \ln k_i^* + RT\,\partial \ln k_i^*/\partial T - R\,\beta \tag{6}$$

$$\Delta\bar{H}_a = RT^2\,\partial \ln k_i^*/\partial T \tag{7}$$

Notice that β ($\equiv \ln \bar{V}_w/V_w$) is assumed to be independent of temperature. In this respect, the RP-18 layer is treated as a solid adsorbent. However, contrary to solid adsorbents, the thermodynamic adsorption data on alkyl silicas may be affected by alterations in the structure of the interface, as will be shown below.

EXPERIMENTAL

Chemicals and adsorbent characterization

The solutes were of the highest available purity. Water was distilled twice and degassed before use by saturation with nitrogen, followed by sonication. The LiChrosorb RP-18 (E. Merck, Darmstadt, F.R.G.) was taken from the same batch as used previously[10] and has an ODS surface concentration equal to 4.4 μmoles/m^2. In view of its large ODS content, the layer may have been slightly polymerized during the silylation reaction.

Apparatus and procedure

The eluent delivery system consisted of an Orlita DMP 1515/3 diaphragm pump and two pulse dampeners in series. The four-port Valco sample valve was equipped with a 3-μl loop. The heat exchanger capillary tube (25 cm × 0.2 mm I.D.) and the column (precision-bore stainless steel, 25 cm × 2.1 mm I.D.) were surrounded by a water-jacket and thermostatted by a Colora cryostat to within 0.05°C. The column temperature was measured with calibrated Anschütz thermometers to 0.1°C. Solute detection was performed with a Coleman M55 UV-visible spectrophotometer. The retention volume of ^2H_2O was monitored with a Waters R401 refractometer detector. After the eluate had been thermostatted at 25°C by means of a heat exchanger, the flow-rate was continuously monitored with a siphon counter (Waters Assoc., Milford, MA, U.S.A.), which was calibrated daily and at any flow-rate. The column was packed by a slurry packing technique. The slurry [10% (w/w) RP-18 in 1-propanol] was degassed and homogenized by sonication, and forced into the column with 300 ml of hexane at 350 atm. Next, 100 ml of acetonitrile and 200 ml of methanol were successively flushed through the column. The weight of adsorbent in the column was 0.442 g.

The void volume of the column, V_0, was determined by picnometry with carbon tetrachloride and *n*-hexane and appeared to be 725 μl. The hexane in the column was replaced by methanol, as described above. At 5°C, about 300 ml of water were required to remove the methanol from the column [verified by means of gas chromatography (GC)]. At higher temperatures, a negligible amount (2 μl in total) of entrapped[15] methanol was released from the RP-18 phase. At the applied column pressures (100–150 atm) the $V_{R,^2H_2O}$ values appeared to be independent of pressure and temperature (5–50°C). Above 50°C a tiny decrease of $V_{R,^2H_2O}$ (about 25 μl) could be inferred from a gradual shift of the UV peak of ^2H_2O (not to be used for absolute V_R measurements). In the range 5–50°C, $V_{R,^2H_2O}$ amounts to 640 μl on the R-layer, and 615 μl on the S-layer at all temperatures (layer notations as in the next section). As S_{BET} = 171 m^2 per g adsorbent[10], $\bar{V}_w/V_w \lesssim 0.04$ in eqn. 4 because of incomplete wetting of the RP-18 layer by water.

Capacity ratio measurements were started after the removal of methanol by water at 5°C and were carried out at 5°-intervals up to 85°C. The solute sample size was $\leqslant$ 5 μg. The shape of the peaks was virtually symmetrical, except for phenol above 75°C. A temperature equilibration period of 3 h appeared to be necessary in order to achieve a long-term reproducibility of the capacity ratios of 1–2%. Capacity ratios were calculated from eqn. 2. For convenience, these k^* data will be denoted by k in the following. It was verified that k is independent of flow-rate in the range 0.3–1.5 ml/min.

RESULTS AND DISCUSSION

Structural changes in the bonded-phase layer of LiChrosorb RP-18

Experimental ln k data of benzene, nitrobenzene and phenol are plotted *versus* $1/T$ in Fig. 1. These plots are comparable with those obtained for phenol or resorcinol on octyl, nonyl and decyl silicas by Gilpin and Squires[12], but our results on LiChrosorb RP-18 strongly deviate from those on laboratory-prepared octadecyl silicas where Gilpin and Sisco[13] obtained essentially linear plots of ln k *versus* 1/T for phenol. Before discussing this dissimilarity, attention is turned first to some features of the retention on LiChrosorb RP-18.

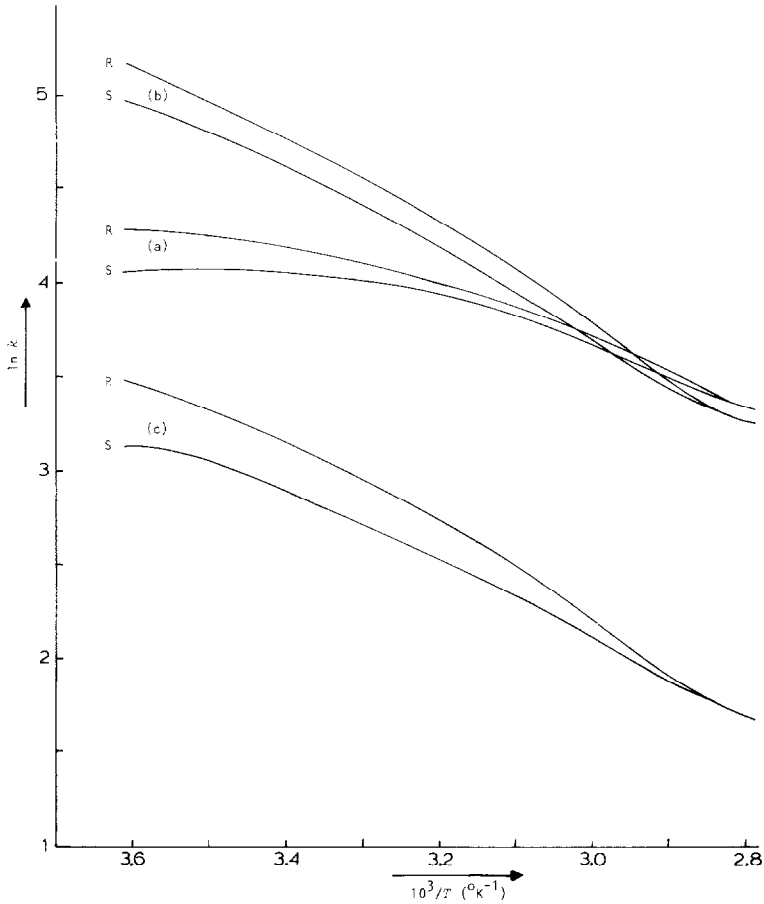

Fig. 1. Plots of ln k *versus* $1/T$ for benzene (a), nitrobenzene (b) and phenol (c) on the R- and the S-layers of LiChrosorb RP-18.

An increase of the column temperature (initially at 5°C) causes a steady decrease of ln k (upper curves in Fig. 1). However, when the column is slowly cooled from 50 to 25°C, the ln k values at 25°C are not in accordance with the upper curves but are, in between the upper and the lower curves. On the other hand, when the column temperature is maintained at 50°C for about 24 h, the k values remain unchanged. Obviously, on heating, some irreversible change of structure in the RP-18 layer occurs, which is counteracted by a stabilizing effect, probably due to hydrophobic association of octadecyl chain ends that are in contact with water. Further heating of the column to $\geqslant 79$°C and successive cooling yields ln k values that lie on the lower curves, whatever temperature changes are further applied, provided that they are sufficiently slow. Apparently, the irreversible phase-transition is finished at 79°C. In the following, the RP-18 layer of the higher and that of the lower adsorptive strength will be denoted as the R- and the S-layer, respectively. The heat-induced alteration in the adsorptive properties of LiChrosorb RP-18 cannot be ascribed to (thermal) decomposition. After flushing the column successively with methanol and

with water (200 ml of each), the k values obtained are within error equal to those obtained in the first measuring cycle. In total three cycles were performed. Thermal stability has also been established by Gilpin and Squires.

As far as the structure of the R-layer is concerned, we agree with previous proposals[12]. It is assumed that in methanol the RP-18 structure is rather chaotic. As a result of the abrupt switch from methanol to water, the RP-18 layer instantly collapses, due to reinforced hydrophobic association, and a rather rough surface layer is formed (Fig. 2A). On heating, the kinetic energy of the alkyl chains increases and the R-layer will gradually expand to a less dense, bristle-like phase (Fig. 2B). According to Gilpin and Squires[12] this configuration is maintained on cooling, and the space among the alkyl chains is occupied by water molecules. However, from an energetic point of view, this picture seems less plausible for RP-18 layers. In our opinion, the bristle phase steadily collapses on cooling to an S-layer with a smooth surface that consists of more or less regularly associated alkyl chains (Fig. 2C). Conclusive evidence for this dynamic behaviour is obtained from the following experimental facts. Significantly larger ln k values were found after rapid cooling from 79 to 10°C than those obtained after very slow cooling, *i.e.*, than those on the lower curves in Fig. 1 at 10°C. Only the k values of phenol are apparently unaffected by the cooling rate. Further, we observed that solute molecules can be trapped in the RP-18 layer on rapid cooling. After a sample injection at 80°C the eluent flow was stopped and the column was abruptly cooled to 25°C. The pump was then actuated again and the solute peaks were recorded. The column was heated to 80°C at zero flow-rate and, finally, the entrapped part of the sample was eluted and recorded. From the peak areas in the two chromatograms and the k values it is estimated that about 20% of the sorbed solute molecules entered the bristle phase to some depth. The remaining 80% of the solute is sorbed into, or quite close to, the interfacial layer between RP-18 and water. Thus, even at high temperatures, solute retention on LiChrosorb RP-18 is mainly controlled by an adsorption mechanism. This unexpected result is attributed to two effects:

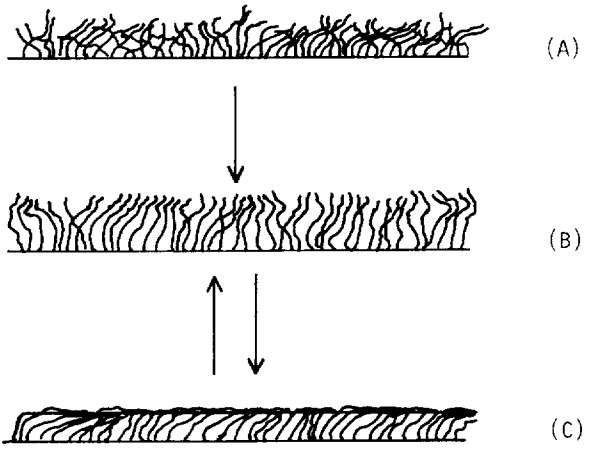

Fig. 2. Schematic illustrations of the R-layer (A), the bristle layer (B) and the S-layer (C) on LiChrosorb RP-18. The layer densities probably differ less than is suggested.

(1) Morel and Serpinet[16] showed that solute partitioning on "molten" RP-18 layers prevails in GC columns at temperatures above 27°C. Below about 7°C, solute molecules are adsorbed on a "crystalline" RP-18 surface. However, a thin coating of a polar liquid, like glycerol, appears to raise the melting range by about 10°C. This stabilization of the crystalline phase has been ascribed to hydrophobic association of alkyl chain ends by the glycerol coating[17]. As it can be reasonably expected that the RP-18 layer is even more strongly stabilized by water, solute adsorption will prevail at still higher temperatures.

(2) Solute sorption from the vapour phase and from water are also different in another respect. In the latter case, the free energy of adsorption is approximately minimal when the total surface area of a non-polar solute molecule and the alkyl layer that loses contact with water molecules on sorption is maximal[10]. As dispersive interactions in water and in the alkyl layer are similar[18], alkane molecules will show little tendency to penetrate the associated RP-18 layer. Complete immersion of polar solute molecules in the alkyl layer is even less likely, because favourable polar interactions with interfacial water molecules would be lost.

According to these considerations, flat adsorption to the S-layer *i.e.*, with an as large as possible portion of the molecular surface exposed to the S-layer, will occur. As the R-layer is assumed to have a slightly diffuse surface structure (see Fig. 2), solute molecules may be partly enclosed by a free alkyl chain end. This improved solute–adsorbent contact probably explains the relatively high adsorptive strength of the R-layer.

Finally, the different retention behaviour on the laboratory-prepared RP-18 adsorbents examined by Gilpin and Sisco[13] and that on LiChrosorb RP-18 will be discussed. From the increase in on-set temperatures of the phase transition with increasing chain length, Gilpin and Squires[12] concluded that a transition in a RP-18 phase in water is not expected below about 140°C. In view of our results, such extrapolation is erroneous. By relating their $[k(\mathrm{R}) - k(\mathrm{S})]/k(\mathrm{R})$ data to the ratio $\%\mathrm{C}/n_c$, *i.e.*, the weight of bound carbon per gram of adsorbent divided by the number of carbon atoms of the alkyl chain, we found that an irreversible transition in the RP-18 layer is not apparent from ln k values as long as $\%\mathrm{C}/n_c \lesssim 0.9$. Because $\%\mathrm{C}/n_c < 0.88$ for the RP-18 phases examined by Gilpin and Sisco[13], it is expected that the R- and S-curves will coincide, as is indeed observed. However, it is true that on LiChrosorb RP-18, $\%\mathrm{C}/n_c = 1.14$, although the specific surface area of the parent silica of the latter is smaller than that used by Gilpin. Obviously, the different retention behaviour on the two adsorbents is connected with the larger surface concentration of alkyl chains on LiChrosorb RP-18.

It is noted that the curvature of the ln k *versus* $1/T$ plots in Fig. 1 need not be connected with a transition in the alkyl layer. For benzene a similar curved plot is obtained for the activity coefficients in water (see eqn. 3), and hence a plot of ln (k/γ^{∞}) *versus* $1/T$ is approximately linear. Therefore, conclusive evidence about the occurrence of structural alterations in bound alkyl layers in water cannot be based on the shape of Van 't Hoff plots, as was suggested by Gilpin and Squires[12].

The influence of the alkyl layer structure on the plate height is not significant. Only phenol gave skewed peaks above 70°C. Probably, residual silanol groups become accessible for adsorption at high temperatures.

Curve fitting results

Taylor's series expansions and T-polynomials were fitted to experimental ln k values at $T \leqslant 348°K$*, and to solubility data of benzene in water (ln $x_{sat.}$) and distribution coefficients of benzene between the perfect vapour phase and water (ln f/x), given by Franks *et al.*[19]. The six constant Taylor's series expansion reads[20]

$$R \ln X = -\frac{\Delta\bar{G}_\theta}{\theta} + \Delta\bar{H}_\theta\left(\frac{1}{\theta} - \frac{1}{T}\right) + \Delta\bar{C}_{p_\theta}\left[\frac{\theta}{T} - 1 + \ln\left(\frac{T}{\theta}\right)\right] +$$

$$+ \frac{\theta}{2}(\partial\Delta\bar{C}_p/\partial T)_\theta\left[\frac{T}{\theta} - \frac{\theta}{T} - 2\ln\left(\frac{T}{\theta}\right)\right] +$$

$$+ \frac{\theta^2}{12}(\partial^2\Delta\bar{C}_p/\partial T^2)_\theta\left[\left(\frac{T}{\theta}\right)^2 - 6\frac{T}{\theta} + 3 + 2\frac{\theta}{T} + 6\ln\left(\frac{T}{\theta}\right)\right] +$$

$$+ \frac{\theta^3}{72}(\partial^3\Delta\bar{C}_p/\partial T^3)_\theta\left[\left(\frac{T}{\theta}\right)^3 - 6\left(\frac{T}{\theta}\right)^2 + 18\frac{T}{\theta}\right.$$

$$\left. - 10 - 3\frac{\theta}{T} - 12\ln\left(\frac{T}{\theta}\right)\right] \tag{8}$$

and can be rearranged to the six-term relation:

$$R \ln X = A + BT^{-1} + C \ln T + DT + ET^2 + FT^3 \tag{9}$$

The T-polynomial of $m + 1$ terms is given by:

$$R \ln X = \sum_{i=0}^{m} a_i T^i \tag{10}$$

In these equations X denotes $kV_w/\bar{V}_w$, $x_{sat.}$ or f/x; θ is a reference temperature (°K) and $m \leqslant 6$ (eqn. 10) in this work. The minimum numbers of terms in eqns. 8 and 10 required for an optimum fit to the data is estimated by means of the usual criteria: (1) the standard error of fit (s) should be minimal; (2) if s^2 of a $z + 1$-term polynomial fit is not significantly smaller than that of a z-term polynomial fit (to be judged from an appropriate F-test[20] at a confidence level of 95%), the z-term equation is preferred. Standard errors of fit for various numbers of terms involved in eqns. 8 and 10 are given in Table I. From the results the following conclusions can be drawn:

(i) When two terms are involved, eqn. 10 offers the best fit. Current chromatographic practice for obtaining enthalpy data from Van 't Hoff plots (eqn. 8 with $\Delta\bar{C}_{p_a} = 0$) is not recommended when water is used as eluent.

* Data at $T \geqslant 352°K$, *i.e.*, on the bristle phase, are not employed in order to avoid inconsistent curve-fitting results.

TABLE I

STANDARD ERRORS OF FIT, s, FOR VARIOUS NUMBERS OF TERMS IN EQNS. 8 AND 10 FOR SEVERAL DATA SERIES FOR BENZENE, NITROBENZENE AND PHENOL, AND THE NUMBER OF TERMS FOR AN OPTIMAL FIT TO THE DATA, z

Solute	*Parameter*	*n*	*Eqn.*	$s \cdot 10^3$ *for various nos. of terms in eqns. 8 and 10*						*z*
				2	*3*	*4*	*5*	*6*	*7*	
Benzene	ln (f/x)	31	8	61	6.4	6.5	6.6	4.4		6
			10	10	9.7	6.5	6.5	4.4	4.5	
	ln $x_{sat.}$	31	8	53	6.1	6.2	6.2	4.6		6
			10	46	7.2	6.2	6.1	4.6	4.7	
	ln k (R)	17	8	56	14.1	14.2	14.3	14.9		3
			10	41	13.7	14.2	14.3	14.9	15.5	
	ln k (S)	22	8	73	16.9	14.0	10.8	11.1		5
			10	61	20.3	13.3	11.1	11.2	11.3	
Nitrobenzene	ln k (R)	16	8	41	11.6	11.9	11.0	10.5		6
			10	14	11.8	11.8	10.8	10.7	9.0	
	ln k (S)	21	8	29	12.1	12.2	11.2	9.0		6
			10	13	12.2	12.1	10.9	9.1	9.1	
Phenol	ln k (R)	14	8	58	17.8	15.6	11.1	11.6		5
			10	29	19.4	14.7	11.4	11.5	12.1	
	ln k (S)	23	8	43	19.7	17.8	18.3	14.2		6
			10	23	20.4	17.9	18.4	14.5	14.2	

(ii) When three or more terms are involved, eqn. 8 (or 9) fits the data equally well (or even better) than eqn. 10. Franks *et al.*[19] claimed that eqn. 10 is superior but omitted to adduce arguments in support of this conclusion. Apart from that, our enthalpies and heat capacities from ln (f/x) data obtained with eqns. 8 and 10 are in excellent agreement with their results.

(iii) The optimum number of terms, z, in eqns. 8 and 10 is given in the last column of Table I and appears to range from three to six for the ln k data series.

TABLE II

STANDARD PARTIAL MOLAR EXCESS FREE ENERGIES, ENTHALPIES, ENTROPIES AND HEAT CAPACITIES FOR BENZENE IN WATER, AND THEIR STANDARD DEVIATIONS

T (°C)	$\Delta\bar{G}^E \pm s$ (cal/mole)	$\Delta\bar{H}^E \pm s$ (kcal/mole)	$\Delta\bar{S}^E \pm s$ (cal/mole · °K)	$\Delta\bar{C}_p^E \pm s$ (cal/mole · °K)
10	4403 ± 1	−0.30 ± 0.07	−16.6 ± 0.2	−17 ± 23
15	4486 ± 1	−0.21 ± 0.04	−16.3 ± 0.1	44 ± 9
20	4565 ± 1	0.10 ± 0.05	−15.2 ± 0.2	76 ± 5
25	4638 ± 1	0.51 ± 0.03	−13.9 ± 0.1	84 ± 6
30	4703 ± 1	0.92 ± 0.03	−12.5 ± 0.1	77 ± 5
35	4763 ± 1	1.27 ± 0.03	−11.4 ± 0.1	61 ± 4
40	4817 ± 1	1.53 ± 0.03	−10.5 ± 0.1	45 ± 4
45	4868 ± 1	1.72 ± 0.03	− 9.9 ± 0.1	34 ± 5
50	4916 ± 1	1.90 ± 0.04	− 9.4 ± 0.1	37 ± 6
55	4962 ± 1	2.13 ± 0.05	− 8.6 ± 0.2	61 ± 6
60	5002 ± 1	2.55 ± 0.05	− 7.4 ± 0.2	112 ± 14

TABLE III

APPARENT PARTIAL MOLAR ADSORPTION DATA FOR BENZENE, NITROBENZENE AND PHENOL FROM WATER ON THE INTERFACIAL R- AND S-LAYERS OF LICHROSORB RP-18, AND THEIR STANDARD DEVIATIONS

$R\beta \lesssim -6.4$ cal/mole · °K, monolayer adsorption model.

T(°C)	$\Delta\bar{G}_a - RT\beta$ (cal/mole)		$\Delta\bar{H}_a$ (kcal/mole)		$\Delta\bar{S}_a + R\beta$ (cal/mole · °K)		$\Delta\bar{C}_{pa}$ (cal/mole · °K)	
	R	*S*	*R*	*S*	*R*	*S*	*R*	*S*
Benzene								
10	−2395 ± 3	−2287 ± 3						
15	−2419 ± 3	−2328 ± 3	−1.14 ± 0.08	−0.09 ± 0.08	4.5 ± 0.3	7.8 ± 0.3		− 47 ± 18
20	−2440 ± 3	−2365 ± 3	−1.38 ± 0.06	−0.39 ± 0.07	3.6 ± 0.2	6.8 ± 0.2		− 71 ± 10
25	−2456 ± 3	−2395 ± 2	−1.63 ± 0.05	−0.79 ± 0.08	2.8 ± 0.2	5.4 ± 0.3		− 88 ± 6
30	−2467 ± 3	−2418 ± 3	−1.88 ± 0.04	−1.25 ± 0.07	1.9 ± 0.1	3.9 ± 0.2		− 97 ± 6
35	−2475 ± 3	−2434 ± 3	−2.13 ± 0.03	−1.74 ± 0.06	1.1 ± 0.1	2.3 ± 0.2	−50 ± 3	− 99 ± 8
40	−2479 ± 3	−2441 ± 3	−2.38 ± 0.03	−2.22 ± 0.06	0.3 ± 0.1	0.7 ± 0.2		− 93 ± 8
45	−2478 ± 3	−2441 ± 3	−2.62 ± 0.04	−2.66 ± 0.07	− 0.5 ± 0.1	− 0.7 ± 0.2		− 80 ± 7
50	−2474 ± 3	−2434 ± 3	−2.87 ± 0.05	−3.01 ± 0.08	− 1.2 ± 0.2	− 1.8 ± 0.3		− 60 ± 6
55	−2466 ± 3	−2423 ± 3	−3.12 ± 0.07	−3.25 ± 0.08	− 2.0 ± 0.2	− 2.5 ± 0.3		− 33 ± 7
60	−2454 ± 3	−2410 ± 3	−3.37 ± 0.08	−3.33 ± 0.08	− 2.7 ± 0.2	− 2.8 ± 0.2		2 ± 14

Nitrobenzene								
10	−2830 ± 4	−2732 ± 3						
15	−2811 ± 4	−2712 ± 3	−4.05 ± 0.14	−4.05 ± 0.09	− 4.3 ± 0.5	− 4.6 ± 0.3	−47 ± 50	− 40 ± 19
20	−2787 ± 4	−2687 ± 2	−4.21 ± 0.14	−4.15 ± 0.10	− 4.9 ± 0.5	− 5.0 ± 0.3	−23 ± 19	− 6 ± 9
25	−2763 ± 3	−2662 ± 2	−4.31 ± 0.13	−4.15 ± 0.08	− 5.2 ± 0.4	− 5.0 ± 0.3	−17 ± 15	3 ± 12
30	−2736 ± 3	−2637 ± 2	−4.41 ± 0.10	−4.15 ± 0.06	− 5.5 ± 0.3	− 5.0 ± 0.2	−25 ± 17	− 5 ± 11
35	−2707 ± 3	−2612 ± 2	−4.57 ± 0.10	−4.22 ± 0.07	− 6.0 ± 0.3	− 5.2 ± 0.2	−39 ± 14	− 24 ± 9
40	−2675 ± 3	−2585 ± 2	−4.81 ± 0.11	−4.39 ± 0.08	− 6.8 ± 0.4	− 5.8 ± 0.3	−56 ± 10	− 44 ± 7
45	−2639 ± 3	−2551 ± 3	−5.12 ± 0.10	−4.65 ± 0.08	− 7.8 ± 0.3	− 6.6 ± 0.2	−68 ± 13	− 60 ± 7
50	−2597 ± 3	−2519 ± 3	−5.47 ± 0.10	−4.97 ± 0.07	− 8.9 ± 0.3	− 7.6 ± 0.2	−71 ± 18	− 63 ± 12
55	−2550 ± 3	−2478 ± 3	−5.80 ± 0.13	−5.25 ± 0.09	− 9.9 ± 0.4	− 8.4 ± 0.3	−58 ± 18	− 45 ± 12
60	−2499 ± 3	−2435 ± 3	−6.01 ± 0.17	−5.37 ± 0.11	−10.6 ± 0.5	− 8.8 ± 0.3	−23 ± 15	1 ± 11
Phenol								
10	−1886 ± 5	−1739 ± 4						
15	−1863 ± 5	−1722 ± 4	−3.20 ± 0.10	−3.13 ± 0.13	− 4.7 ± 0.3	− 4.9 ± 0.5	−17 ± 23	−137 ± 29
20	−1839 ± 5	−1694 ± 4	−3.37 ± 0.10	−3.55 ± 0.15	− 5.2 ± 0.3	− 6.3 ± 0.5	−45 ± 13	− 41 ± 14
25	−1811 ± 4	−1662 ± 4	−3.65 ± 0.11	−3.62 ± 0.12	− 6.2 ± 0.4	− 6.6 ± 0.4	−66 ± 7	4 ± 17
30	−1777 ± 4	−1629 ± 4	−4.01 ± 0.11	−3.57 ± 0.10	− 7.4 ± 0.4	− 6.4 ± 0.3	−79 ± 7	10 ± 17
35	−1737 ± 4	−1598 ± 4	−4.42 ± 0.09	−3.56 ± 0.11	− 8.7 ± 0.3	− 6.4 ± 0.4	−83 ± 10	− 9 ± 13
40	−1690 ± 4	−1565 ± 4	−4.84 ± 0.07	−3.68 ± 0.12	−10.1 ± 0.2	− 6.8 ± 0.4	−80 ± 10	− 39 ± 11
45	−1636 ± 3	−1529 ± 4	−5.21 ± 0.08	−3.95 ± 0.11	−11.2 ± 0.3	− 7.6 ± 0.3	−69 ± 9	− 68 ± 15
50	−1578 ± 3	−1488 ± 4	−5.52 ± 0.10	−4.33 ± 0.11	−12.2 ± 0.3	− 8.8 ± 0.3	−50 ± 7	− 82 ± 19
55	−1515 ± 3	−1441 ± 4	−5.70 ± 0.10	−4.72 ± 0.15	−12.8 ± 0.3	−10.0 ± 0.4	−23 ± 8	− 67 ± 18
60	−1451 ± 3	−1389 ± 4	−5.73 ± 0.10	−4.94 ± 0.18	−12.8 ± 0.4	−10.7 ± 0.5	12 ± 14	− 11 ± 18

Because z is susceptible to small systematic experimental errors, this result is not surprising. Possible artifacts due to this uncertainty in z (± 1) can be avoided by omitting computer results within the lower 10° and the upper 15° of the examined temperature range. The s values obtained for the various z-term polynomials are in accord with estimates of the experimental error (0.5% of $x_{sat.}$ and 1–2% of k).

Smoothed $\Delta\bar{G}$, $\Delta\bar{H}$, $\Delta\bar{S}$ and $\Delta\bar{C}_p$ values for the various data series as well as their standard deviations, evaluated from eqn. 8, are given in the Tables II and III. It should be borne in mind that, due to the dynamic behaviour of both RP-18 layers, ln k values at different temperatures refer to more or less different adsorbent structures. Consequently, the thermodynamic adsorption data on these layers will deviate from those on rigid adsorbents of a similar chemical constitution. For that reason, we have occasionally assigned the predicate "apparent" to our data.

Enthalpy–entropy correlation

It is easily shown from the Gibbs equation, $\Delta\bar{G}_a = \Delta\bar{H}_a - T\Delta\bar{S}_a$, that effects of a temperature change on $\Delta\bar{H}_a$ and on $\Delta\bar{S}_a$ are related by the equation:

$$\partial\Delta\bar{H}_a/\partial\Delta\bar{S}_a = T \tag{11}$$

As the experimental error of $\Delta\bar{G}_a$ data is relatively small, this equation also relates the errors of $\Delta\bar{H}_a$ to those of $\Delta\bar{S}_a$. When $\Delta\bar{H}_a$ is plotted *versus* $\Delta\bar{S}_a$ for a series of solutes and the slope of this plot is close to the experimental temperature, T, it is often hard to establish whether such a correlation is a consequence of physico-chemical causes or merely due the (usually large) experimental errors. Therefore, Krug *et al.*[21,22] proposed to correlate $\Delta G/T$, instead of ΔS, with ΔH data

$$\Delta\bar{G}_a/T = \Delta\bar{H}_a\left(\frac{1}{T} - \frac{1}{\tau}\right) + \Delta\bar{G}_a\,(T = \tau)/\tau \tag{12}$$

where τ is the isokinetic (or compensation) temperature. In eqn. 12 $\Delta\bar{G}_a/T$ and $\Delta\bar{G}_a/\tau$ at $T = \tau$ may be replaced by the corresponding $-R \ln k$ data (see eqn. 5). Because the $R \ln k$ *vs.* $\Delta\bar{H}_a$ correlations for our experimental data are poor on both the R- and S-layers, no more can be concluded from eqn. 12 than at least one of the three solutes shows a deviating retention behaviour. From eqn. 11 (and eqns. 5–7) it is clear that enthalpy data offer the best prospect for improvement of the description of solute adsorption in the RP-18–water system.

Influence of the structure of the RP-18–water interface

In Fig. 3, $\Delta\Delta\bar{H}_a \equiv \Delta\bar{H}_a$ (R) $- \Delta\bar{H}_a$ (S) data are plotted *versus* T. Obviously, the shapes of the curves are connected with the polarity of the solutes. The $\Delta\Delta\bar{H}_a$ values of nitrobenzene steadily decrease with increasing temperature, those of the very polar phenol go through a minimum, whereas those of the non-polar benzene tend to a maximum. These results clearly illustrate the pronounced effect of the layer structure on the enthalpic contribution to solute retention. The relatively large $-\Delta\Delta\bar{H}_a$ value of benzene at 15°C may be due to the better solute–adsorbent contact on the R-layer. At higher temperatures the R- and the S-layers are more alike and, accordingly, $-\Delta\Delta\bar{H}_a$ becomes smaller. The influence of (changes of) the layer struc-

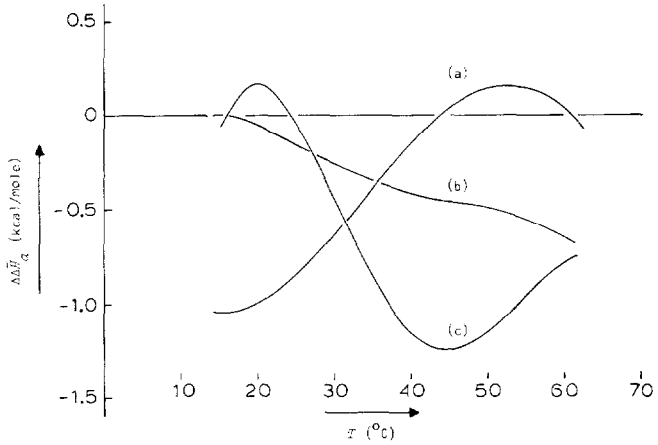

Fig. 3. $\Delta\Delta\bar{H}_a \equiv \Delta\bar{H}_a$ (R) $- \Delta\bar{H}_a$ (S) as a function of temperature for benzene (a), nitrobenzene (b) and phenol (c). The standard errors of the data described by the curves are $\leqslant 0.2$ kcal/mole.

ture on $\Delta\bar{H}_a$ values of polar solutes is far more complex. Polar interactions in the interface may deviate from those in water[14]. Note that the characteristic curve pattern in Fig. 3 is not apparent from the curves in Fig. 1. This is a result of enthalpy/entropy compensation effects. Obviously, the extent of compensation depends on the solute polarity.

Influence of cavity formation, hydrophobic hydration and solute polarity

In order to obtain a better insight into the adsorption of non-polar solutes from water, the phenomena that attend the transfer of benzene molecules from benzene to water will be reviewed briefly. The standard partial molar excess free energy connected with that process is given by:

$$\Delta\bar{G}^E \equiv RT \ln \gamma^\infty \approx -RT \ln x_{sat.} \tag{13}$$

As the mole fractional solubility of benzene in water, $x_{sat.}$, is very small, concentration effects on the activity coefficient, γ^∞, may be neglected. At 25°C, $\Delta\bar{G}^E = 4.64$ kcal/mole, $\Delta\bar{H}^E = 0.51$ kcal/mole and $\Delta\bar{S}^E = -13.9$ cal/mole · °K (see Table II). The large $-\Delta\bar{S}^E$ values of non-polar solutes, like benzene, in water have been ascribed to a diminished freedom of motion of the water molecules in the hydration shell around a solute molecule, relative to that in the water bulk[23]. As $\Delta\bar{H}^E$ is rather small, the strongly positive $\Delta\bar{G}^E$ values of benzene and other non-polar molecules are mainly due to entropy effects on this hydrophobic hydration in water[24–26]. On adsorption, a number of water molecules are transferred from the hydration shell to the less-ordered bulk water. Accordingly, positive $\Delta\bar{S}_a$ and negative $\Delta\bar{G}_a$ values are expected and obtained (see Table III, benzene), and adsorption from water is essentially an entropy-driven process[25]. As it is expected that the order in the hydration shell will decrease with increasing temperature, it is not surprising that $\Delta\bar{S}^E$ and $\Delta\bar{H}^E$ increase with temperature and that $\Delta\bar{C}_p^E$ is positive (see Table II). Accordingly, $\Delta\bar{S}_a$ and $\Delta\bar{H}_a$ will decrease with increasing temperature and $\Delta\bar{C}_{p_a}$ is negative, as is indeed observed on both layers (see Table III, benzene).

Although this reasoning ostensibly agrees with the experimental results, it has a serious shortcoming in that it ignores the contribution of cavity formation to the excess data. Shinoda[27] obtained the following rough estimates for benzene at 25°C: $\Delta\bar{H}_{\text{cav.}} \approx 8.1$ kcal/mole and $\Delta\bar{S}_{\text{cav.}} \approx 7.2$ cal/mole · °K. Combination with the excess data yields the contribution of hydrophobic hydration: $\Delta\bar{H}_{\text{h}} \approx -7.6$ kcal/mole and $\Delta\bar{S}_{\text{h}} \approx -21.1$ cal/mole · °K, giving $\Delta\bar{G}_{\text{h}} \approx -1.3$ kcal/mole. Note that these substantial contributions of $\Delta\bar{S}_{\text{h}}$ and $\Delta\bar{H}_{\text{h}}$ largely cancel in the $\Delta\bar{G}^{\text{E}}$ data. Complete enthalpy/entropy compensation of hydration effects has been predicted by Ben-Naim[28]. Also, Patterson and Barbe[29] have discussed compensation effects on order/disorder phenomena and, in essence, the present results from Shinoda's model confirm their conclusions. Evidently, the major driving force for hydrophobic benzene–adsorbent interaction originates from the free energy of cavity formation ($\Delta\bar{G}_{\text{cav.}} \approx 5.95$ kcal/mole from the above data). As part of the solute–adsorbent complex loses contact with water, $\Delta\bar{G}_{\text{a}}$ will be negative. Hydrophobic hydration is clearly not the impetus for solute adsorption. Notice that this conclusion is just the opposite to that implied in the first-mentioned trend of thought.

Next, let us consider the temperature dependence of the excess data more closely. In Fig. 4, $\Delta\bar{G}^{\text{E}}$, $\Delta\bar{H}^{\text{E}}$, $T\Delta\bar{S}^{\text{E}}$ and $\Delta\bar{C}_p^{\text{E}}$ data, given in Table II, are plotted *versus* T. The increase of $\Delta\bar{H}^{\text{E}}$ (and $T\Delta\bar{S}^{\text{E}}$) with temperature is due to the steady removal of order in the hydration shells around the benzene molecules in water. The decrease of $\Delta\bar{C}_p^{\text{E}}$ within the 25–48°C range is connected with a transition in the water structure that causes an increase of the number of water molecules in the "ordered" hydration shells[19]. As a result, the $\Delta\bar{H}^{\text{E}}$ and $T\Delta\bar{S}^{\text{E}}$ curve shows an inflection point at about 48°C. Note that the characteristic sigmoidal shape of these curves is no longer apparent from the $\Delta\bar{G}^{\text{E}}$ curve. This confirms that effects of structural changes in the bulk water on the hydrophobic hydration completely cancel in the excess free energy[28].

The above results can be related to the adsorption data by considering the excess data for the RP-18–water interfaces (denoted by index a/w). The relevant data are obtained from the equation

$$\Delta\bar{Y}^{\text{E}}_{\text{a/w}} = \Delta\bar{Y}^{\text{E}} + \Delta\bar{Y}_{\text{a}} \tag{14}$$

where Y denotes G, H, S or C_p. They represent (apparent) partial molar quantities for the transfer of an infinitely small amount of benzene from benzene to the RP-18–water interface. Interestingly, the $\Delta\bar{C}^{\text{E}}_{p_{\text{a/w}}}$ and $\Delta\bar{H}^{\text{E}}_{\text{a/w}}$ curves have analogously sigmoidal shapes as those for the corresponding excess data in the bulk water (Fig. 4). Association of benzene molecules with the R- and S-layers results into two $\Delta\bar{C}^{\text{E}}_{p_{\text{a/w}}}$ curves that run nearly parallel to the $\Delta\bar{C}_p^{\text{E}}$ curve within the transition region of water. This result is compatible with solute adsorption at the interface of the RP-18 layers. As our $\Delta\bar{C}_{p_{\text{a}}}$ data do not show a characteristic relative maximum at about 48°C, the effects of the transition in water on the adsorption data cannot be established. But, if present, these effects are compensated in $\Delta\bar{G}^{\text{E}}_{\text{a/w}} - RT\beta$ ($\equiv RT \ln \gamma^{\infty}/k$), which increase almost linearly with temperature (see Fig. 4). Interestingly, $\partial \ln (\gamma^{\infty}/k)/\partial T$ appears to be very small, particularly on the S-layer (about 0.004 per °K). This clearly illustrates the importance of eluent effects on solute adsorption. Mean $\Delta\bar{H}^{\text{E}}_{\text{a/w}}$ values on both layers appear to be independent of temperature within

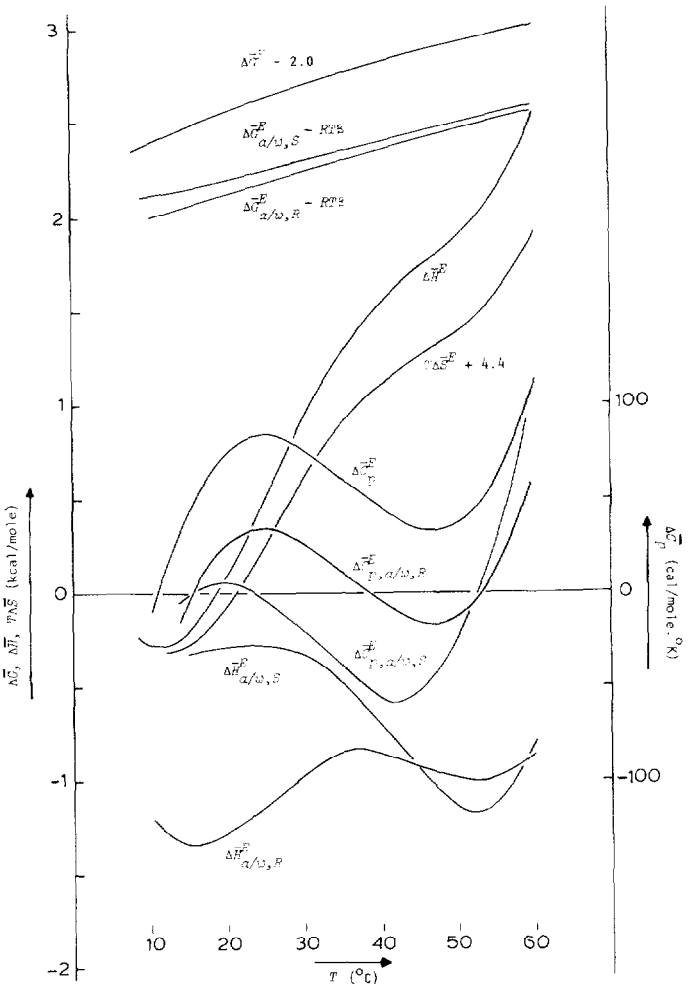

Fig. 4. $\Delta\bar{G}^{E}$, $\Delta\bar{H}^{E}$, $T\Delta\bar{S}^{E}$ and $\Delta\bar{C}_{p}^{E}$ for benzene in water, and $\Delta\bar{G}_{a/w}^{E} - RT\beta$, $\Delta\bar{H}_{a/w}^{E}$ and $\Delta\bar{C}_{p_{a/w}}^{E}$ for benzene (transfer from benzene to the R- or S-interface of LiChrosorb RP-18–water) as a function of temperature. The standard errors of the plotted data are $\leqslant$0.15 kcal/mole (ΔH and $T\Delta S$) or $\leqslant$25 cal/mole · °K (ΔC_p).

0.4 kcal/mole. According to Shinoda's concept (with $\Delta\bar{C}_{p_{\text{cav.}}} = 0$ cal/mole · °K), this implies that the observed decrease of $\Delta\bar{H}_{a}$ with increasing temperature largely originates from the increase of $\Delta\bar{H}_{h}$ (reduction in order in the hydration shell). Of course, alteration of the adsorbent structure will affect $\Delta\bar{H}_{a}$ as well. Analogously, we have pointed out that the decrease of $\Delta\bar{G}_{a}$ and $T\Delta\bar{S}_{a}$ with increasing temperature is governed by the increase of $\Delta\bar{G}^{E}$ and $T\Delta\bar{S}^{E}$, respectively.

From the foregoing it is concluded that cavity formation and hydrophobic hydration effects in the bulk water significantly contribute to $\Delta\bar{S}_{a}$, $\Delta\bar{H}_{a}$ and $\Delta\bar{C}_{p_{a}}$. But the values of $\Delta\bar{G}_{a}$ are mainly governed by the partial release of the positive free energy of cavity formation of benzene in the mobile eluent. A more sophisticated

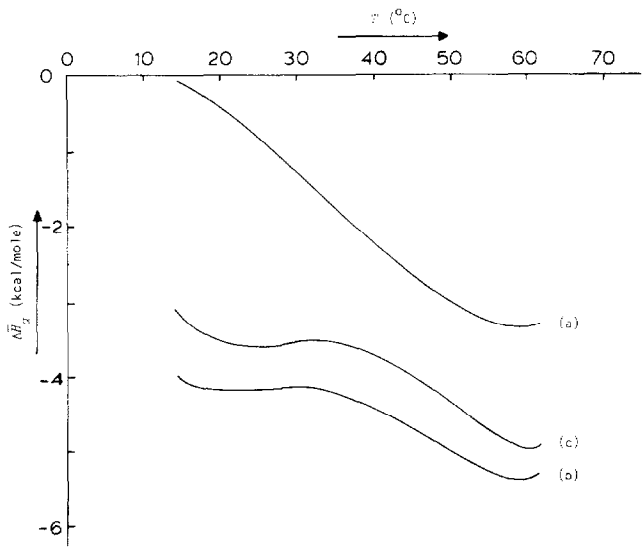

Fig. 5. $\Delta\bar{H}_a$ values of benzene (a), nitrobenzene (b) and phenol (c) on the S-layer of LiChrosorb RP-18 in water as a function of temperature.

model is required to estimate the latter more accurately. The rather simple description of the adsorption data in terms of excess data is connected with our choice of the standard state of the adsorbed solute, *i.e.*, the pure bulk solute[10].

Comparison of the $\Delta\bar{H}_a$ values of nitrobenzene and phenol with those of benzene (see Table III) suggests that the polar NO_2 and OH groups contribute considerably to the (apparent) enthalpy in favour of adsorption, even at the less perturbed S-layer–water interface (see Fig. 5). But these contributions are largely offset (for nitrobenzene) or even overshadowed (for phenol) by negative entropy increments.

Because of their "apparent" character, the results have been described, rather than explained in detail, in the foregoing discussion. In our opinion, this restriction may be appropriate to other dense RP bonded phase–water systems. Recently, a more rigorous treatment of adsorption data in such systems has been outlined by Elkoshi and Grushka[30]. However, it is questionable whether the necessary requirements concerning bonded phase rigidity and absence of accessible silanol sites, presupposed in their interesting approach, can be simultaneously fulfilled. It is worth noting that adsorption and hydrophobic interaction should properly be distinguished[30].

The occurrence of reversible transitions or structural alterations is not exceptional in dense, bonded-phase layers. Morel and Serpinet[16,17] examined transitions on alkyl layers on silica in GC columns. Riedo *et al.*[31] observed transitions on mixed crystal phases, consisting of bonded alkyl and *n*-alkane chains. Kessaissia *et al.*[32] reported low-temperature transitions on moderately dense alkyl layers and associated them with glassy transitions in semi-crystalline polythene. In various nitrophenylaminobutyl layers on silica the extent of association between the polar ligand groups appears to depend on the column temperature and on the eluent polarity[33].

CONCLUSIONS

When (pure) methanol in a LiChrosorb RP-18 column is abruptly removed by water, a "rough" interfacial RP-18–water layer of relatively high adsorptive strength is obtained. On heating at temperatures up to 79°C, this layer shows an irreversible transition to a more or less ordered, bristle-like configuration. On cooling, this bristle phase reversibly collapses to a "smooth" layer of regularly associated RP-18 chains, which shows a relatively low adsorptive strength. Even on the less dense bristle phase, solute adsorption into (or close to) the RP-18–water interface prevails. Results on octyl, nonyl, decyl and octadecyl silicas indicate that irreversible phase transitions are only apparent at a sufficiently high surface concentration of bound alkyl chains.

The ln k *versus* $1/T$ plots of benzene, nitrobenzene and phenol are curved for both the "rough" and the "smooth" RP-18 layer. These ln k values are equally well described by Taylor's series expansions and by T-polynomials of an equal number of terms ($\geqslant 3$).

Apparent enthalpic and entropic contributions to the solute retention strongly depend on the structure of the RP-18–water interface. This effect appears only partly to cancel in the free energies of adsorption. The values of the free energy of adsorption of benzene are mainly governed by the (partial) release of the free energy of cavity formation in the bulk water. Cavity formation as well as hydrophobic hydration effects in the bulk water significantly contribute to the enthalpy and heat capacity of adsorption. In comparison with benzene, both nitrobenzene and phenol show strongly negative (apparent) adsorption enthalpies and entropies.

A rigorous quantitative interpretation of adsorption data on alkyl bonded phases requires a detailed knowledge of the surface structure of these phases.

ACKNOWLEDGEMENT

We are indebted to Dr. J. C. van Miltenburg who kindly placed the computer programs at our disposal.

REFERENCES

1 J. H. Knox and G. Vasvari, *J. Chromatogr.*, 83 (1973) 181.
2 H. Colin, J. C. Diez-Maza, G. Guiochon, T. Czajkowska and I. Miedziak, *J. Chromatogr.*, 167 (1978) 41.
3 H. Colin and G. Guiochon, *J. Chromatogr.*, 158 (1978) 183.
4 H. Colin, J. C. Diez-Maza, G. Guiochon, R. D. Suits, T. P. Waalkens and E. Borek, *J. Chromatogr.*, 150 (1978) 455.
5 Gy. Vigh and Z. Varga-Puchony, *J. Chromatogr.*, 196 (1980) 1.
6 W. Melander, D. E. Campbell and Cs. Horváth, *J. Chromatogr.*, 158 (1978) 215.
7 W. Melander, J. Stoveken and Cs. Horváth, *J. Chromatogr.*, 199 (1980) 35.
8 W. Melander, B.-K. Chen and Cs. Horváth, *J. Chromatogr.*, 185 (1979) 99.
9 C. M. Riley, E. Tomlinson and T. M. Jefferies, *J. Chromatogr.*, 185 (1979) 197.
10 W. E. Hammers, G. J. Meurs and C. L. de Ligny, *J. Chromatogr.*, 246 (1982) 169.
11 H. E. Slaats, W. Markowski, J. Fekete and H. Poppe, *J. Chromatogr.*, 207 (1981) 299.
12 R. K. Gilpin and J. A. Squires, *J. Chromatogr. Sci.*, 19 (1981) 195.
13 R. K. Gilpin and W. R. Sisco, *J. Chromatogr.*, 194 (1980) 285.
14 W. E. Hammers, G. J. Meurs and C. L. de Ligny, *J. Chromatogr.*, 247 (1982) 1.
15 R. K. Gilpin, M. E. Gangoda and A. E. Krishen, *J. Chromatogr. Sci.*, 20 (1982) 345.

16 D. Morel and J. Serpinet, *J. Chromatogr.*, 200 (1980) 95.
17 D. Morel and J. Serpinet, *J. Chromatogr.*, 214 (1981) 202.
18 F. M. Fowkes, *J. Phys. Chem.*, 67 (1963) 2538.
19 F. Franks, M. Gent and H. H. Johnson, *J. Chem. Soc., London*, (1963) 2716.
20 E. C. W. Clarke and D. N. Glew, *Trans. Faraday Soc.*, 62 (1966) 539.
21 R. R. Krug, W. G. Hunter and R. A. Grieger, *J. Phys. Chem.*, 80 (1976) 2335.
22 R. R. Krug, W. G. Hunter and R. A. Grieger, *J. Phys. Chem.*, 80 (1976) 2341.
23 K. Hallenga, J. R. Grigera and H. J. C. Berendsen, *J. Phys. Chem.*, 84 (1980) 2381.
24 G. Némethy and H. A. Scheraga, *J. Phys. Chem.*, 66 (1962) 1773.
25 F. Franks, in F. Franks (Editor), *Water—A Comprehensive Treatise*, Vol. 4, Plenum, New York, 1975, p. 1.
26 C. Tanford, *The Hydrophobic Effect: Formation of Micelles and Biological Membranes*, Wiley, New York, 1973, p. 18.
27 K. Shinoda, *J. Phys. Chem.*, 81 (1977) 1300.
28 A. Ben-Naim, *Water and Aqueous Solutions*, Plenum, New York, 1974, Chs. 7.4 and 8.11.
29 D. Patterson and M. Barbe, *J. Phys. Chem.*, 80 (1976) 2435.
30 Z. Elkoshi and E. Grushka, *J. Phys. Chem.*, 85 (1981) 2980.
31 F. Riedo, M. Czencz, O. Liardon and E. Kováts, *Helv. Chim. Acta*, 61 (1978) 1912.
32 Z. Kessaissia, E. Papirer and J.-B. Donnet, *J. Colloid Interface Sci.*, 79 (1981) 257.
33 W. E. Hammers, A. G. M. Theeuwes, W. K. Brederode and C. L. de Ligny, *J. Chromatogr.*, 234 (1982) 321.